

Supramolecular Structure and Mechanical Characteristics of Ultrahigh-Molecular-Weight Polyethylene–Inorganic Nanoparticle Nanocomposites

T. A. Okhlopkova,[†] R. V. Borisova,[†] L. A. Nikiforov,[†] A. M. Spiridonov,[†]
A. A. Okhlopkova,^{†,*} Dae-Yong Jeong,[‡] and Jin-Ho Cho^{†,§,*}

[†]Department of Chemistry, North-Eastern Federal University, Yakutsk 677000, Russia.

*E-mail: okhlopkova@yandex.ru; jinhcho@mju.ac.kr,

[‡]Department of Materials Science and Engineering, Inha University, Incheon 22212, Korea

[§]Department of Energy and Biotechnology, Myongji University, Yongin 449-728, Korea

Received March 17, 2015, Accepted December 4, 2015, Published online March 30, 2016

We investigated the mechanical properties and structure of polymeric nanocomposites (PNCs) with an ultrahigh-molecular-weight polyethylene (UHMWPE) matrix and aluminum and silicon oxide and nitride nanoparticle (NP) fillers. Mixing with a paddle mixer or by joint mechanical activation in a planetary mill was used for the PNC preparation. Joint mechanical activation afforded PNCs with better mechanical properties than paddle mixing. Scanning electron microscopy suggested that the poorer mechanical properties can be attributed to the disordered regions and imperfect spherulites in the PNC supramolecular structure arising from paddle mixing. The better mechanical properties observed with joint mechanical activation may derive from the uniform NP distribution in the polymer matrix and absence of disordered regions.

Keywords: Ultrahigh-molecular-weight polyethylene, Nanoparticle, Polymer nanocomposite, Mechanical characteristics, Supramolecular structure

Introduction

In recent years, the design and controlled fabrication of nanostructured materials with defined physicochemical properties have gained considerable interest.¹ Nanocomposites based on polymers and inorganic nanoparticles (NPs) have, in particular, demonstrated significant performance in terms of mechanical properties, fire resistance, gas permeability, and electrical conductivity.¹ Conventional sealing, structural, and antifriction materials usually undergo degradation under extreme conditions, such as very low temperatures.² Therefore, materials for application in arctic environments require high strength as well as frost, wear, and corrosion resistance.³

Ultrahigh-molecular-weight polyethylene (UHMWPE) is known to retain its high mechanical and tribotechnical properties at low temperatures, including cryogenic conditions,^{2,4} and under high loading.⁵ UHMWPE also shows excellent self-lubrication properties, high-impact strength, and excellent corrosion and frost resistance in comparison with other polymers. High-density UHMWPE provides good stiffness characteristics and abrasion and chemical resistance.⁵ In addition to the intrinsic characteristics of UHMWPE, its mechanical and tribotechnical properties have been improved by the addition of NP fillers to the polymer.⁶ Briscoe *et al.* demonstrated that the addition of PbO and CuO fillers to high-density polyethylene reduced wear because of the formation of a strong transfer film.⁷ By manufacturing composites of UHMWPE and ceramics such as Al₂O₃, ZrO₂, and Si₃N₄,

biocompatible and wear- and scratch-resistant hybrid materials were successfully fabricated recently and found applications in orthopedics.^{8,9} Metallic silver NPs in UHMWPE demonstrated good wear and tribochemical properties.¹⁰ We have reported different techniques to modify polymer nanocomposites (PNCs)^{2,11} to achieve good tribotechnical and mechanical properties. It is to be noted that the uniform distribution of NPs in the PNCs is critical to achieving high tribotechnical and mechanical properties.¹² Here, we report joint mechanical activation as a unique physical activation method to maximize the uniform distribution of NPs in PNCs. The microstructural and mechanical properties of the PNCs were characterized and related to the homogeneous distribution of the NPs.

Experimental

Materials and PNC Preparation. Powdered UHMWPE (GUR 4120, Ticona, USA) with an average molecular weight of 5×10^6 was used as the polymer matrix. Nanosized oxides and nitrides of Al and Si were used as nanofillers. The physical properties of the NPs are shown in Table 1.

Due to their lower bulk densities than aluminum oxides and nitrides, silicon oxides and nitrides are more fragile and agglomerate less.

The fillers were introduced into the polymer matrix by two different methods. One involved dry mixing of the components in a paddle mixer (SL-1500, Predlojenie, Russia) and

Table 1. Physical properties of the ceramic nanoparticles.

Nanoparticle	Particle size (nm)	Specific surface area (m ² /g)	Phase
Al ₂ O ₃	40	10	α-Al ₂ O ₃
SiO ₂	7–14	200	Amorphous
AlN	25–50	18	96% hexagonal
Si ₃ N ₄	15–25	110	Amorphous

the other utilized joint mechanical activation in a planetary mill (Pulverisette-5, Fritsch, Germany). Although dry mixing with the paddle mixer does not induce any change in the polymer, the planetary mill introduces strong mechanical energy into the polymer and can cause the materials to be in a more active state. The principal schemes underlying the planetary mill and mechanical activation processes are shown in Figure 1.

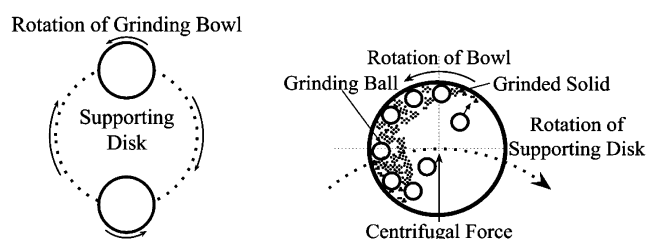
Joint mechanical activation was carried out for 2 min in the planetary mill with a carrier rotation frequency of 400 rpm and drum rotation frequency of 2220 rpm; the centrifugal acceleration developed by the milling bodies was 400 m/s². The PNCs were prepared by hot pressing under 10 MPa for 20 min with prepressing at 4 MPa. The pressing temperature was 175–180 °C and the nanofiller content ranged from 0.1 to 2.0 wt %.

Characterization and Property Measurement. Both the tensile strength and relative elongation at break were measured according to the Russian state standard GOST 11262-80¹³ (Autograph AGS-J, Shimadzu, Kyoto, Japan) at room temperature. The test speed and specimen length were 50 mm/min and 45 mm, respectively. The PNCs were characterized with a scanning electron microscope (SEM, JSM-7800F, JEOL, Akishima, Japan) equipped with energy-dispersive X-ray spectroscopy (EDS, X-MAX 20, Oxford, United Kingdom) for chemical composition analysis. The UHMWPE and composite samples for SEM were prepared by freezing in liquid nitrogen followed by brittle fracture. Polymeric materials melt easily under high energy sources. Therefore, a Schottky-type thermal field emission cathode¹⁴ was sufficient to afford good resolution at low electron acceleration energies.

The crystallinity degrees, sizes of coherent scattering regions, and microdeformations in the PNC crystalline structure were estimated by wide-angle X-ray diffraction (XRD, ARL X'Tra, Thermo Fisher Scientific, Switzerland). The X-ray wavelength was fixed at 0.154056 nm. The scan angle ranged from 3 to 60° in steps of 0.04 and 0.02°, and the scanning rate was 1 s per point. WinXRD (Thermo Fisher) was used for data analysis.

Results and Discussion

The effect of mechanical activation on the properties of the PNCs was evaluated by tensile tests, including the elongation at break and tensile strength as a function of the nanofiller

**Figure 1.** Planetary mill and mechanical activation.

content; results are shown in Figures 2 and 3. The maximum elongation at break was achieved with a nanofiller concentration of 0.5–1 wt %. A further increase in the filler content led to gradual decreases in the physical and mechanical properties.

As shown in Figure 2, the mechanical tests demonstrate the advantage of the mechanical activation of the fillers on a planetary mill.

The elongation at break increased by 35–40% when joint mechanical activation was used. Panin *et al.* demonstrated that the polymer particles deform repeatedly during the mechanically activated processing of UHMWPE.¹² Mechanical activation leads to the flattening of spherical UHMWPE particles to flat flakes with sizes in the range 50–200 microns. Therefore, the mechanical characteristics of UHMWPE are enhanced by an increase in the effective contact area between the polymer molecules. The tensile strength of the PNCs prepared by joint mechanical activation increased by 15–20% in comparison with the PNCs prepared in a paddle mixer (Figure 3).

PNCs with the best mechanical properties were obtained with an optimal concentration of nanofillers.² When the concentration of the nanofillers increased beyond the optimum, the mechanical properties decreased significantly. This can be explained by the adhesive interaction between the polymer and nanofiller within the amorphous phase. Therefore, the nanofiller is effective in the amorphous regions only when its concentration is optimum. The resulting overstress, defective areas, and deformed spherulite structure impact the mechanical properties when an excessively high-nanofiller concentration is used.

The relationship between the mechanical behavior of the PNCs and their microstructures is critical in determining the deformation mechanism of the PNCs.^{15,16} The first stage of deformation is elastic and governed by the mechanical properties of the interlamellar amorphous phase of the PNCs. UHMWPE molecules are particularly important during elastic

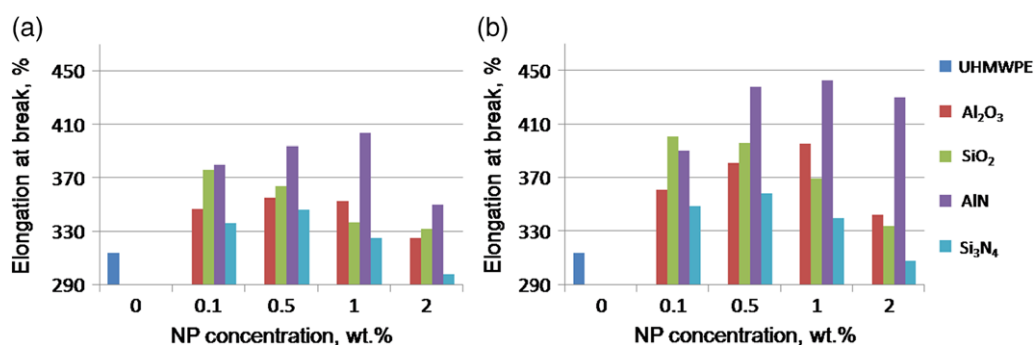


Figure 2. Elongation at break of PNCs prepared by (a) paddle mixer and (b) planetary mill.

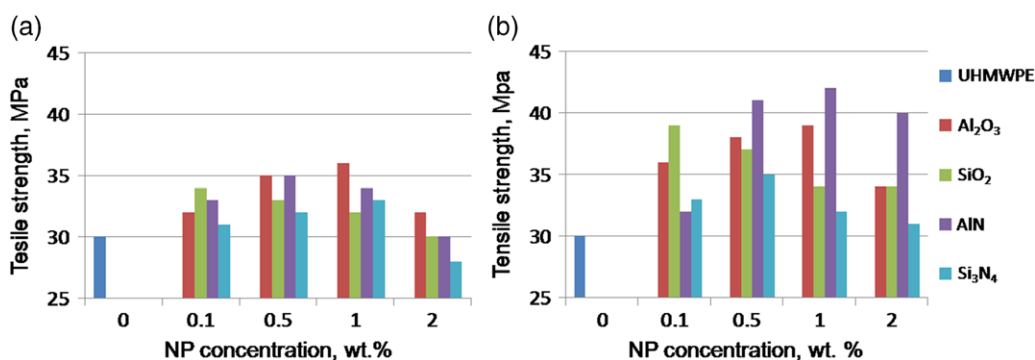


Figure 3. Tensile strength of PNCs prepared by (a) paddle mixer and (b) planetary mill.

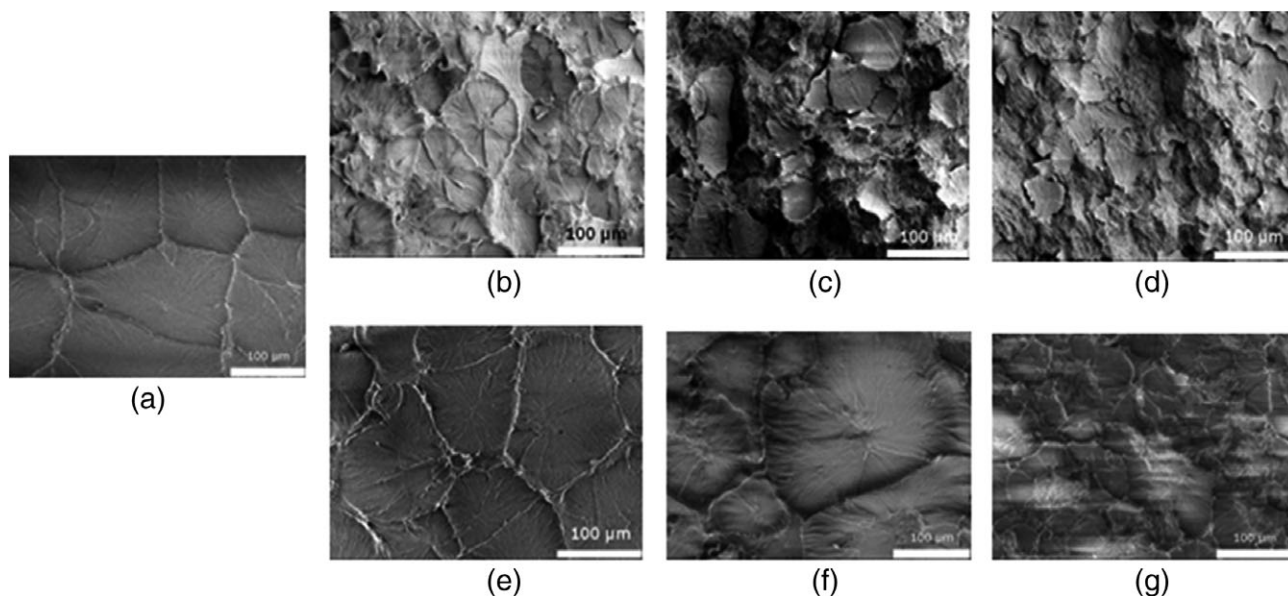


Figure 4. SEM images of (a) initial UHMWPE and UHMWPE with various additives prepared in a paddle mixer (b) 0.5 wt % SiO₂; (c) 1.0 wt % SiO₂; and (d) 2.0 wt % SiO₂; or mixed in a planetary mill (e) 0.5 wt % SiO₂; (f) 1.0 wt % SiO₂; and (g) 2.0 wt % SiO₂.

deformation because they transmit the stress throughout the supramolecular structure. The second stage of deformation occurs in the spherulites and is non-elastic.^{15,16} The SEM images in Figure 4 were obtained to evaluate the supramolecular structure of the PNCs.

Here, the SEM images in Figure 4(b)–(d) were acquired from samples prepared in the paddle mixer and those in Figure 4(e)–(g) represent samples produced by joint mechanical activation in the planetary mill. As shown in Figure 4, joint mechanical activation leads to a more uniform distribution of

the filler in the polymer matrix than that seen in composites made in a paddle mixer. This uniform dispersion of the nanofiller in the polymer matrix is critical for the development of PNCs because a uniform distribution enhances mechanical and tribotechnical characteristics. These PNCs with uniform filler distribution also exhibit other desirable properties, such as good fire resistance, gas permeability characteristics, and electrical conductivity.¹⁷

In addition to their mechanical properties, as shown in Figure 4, the crystallization behavior of the PNCs differs depending on the composite preparation method. Paddle mixing afforded relatively perfect spherulite shapes only at lower nanofiller concentrations (0.1–0.5 wt %), as in Figure 4(b). This spherulite morphology did not appear at higher nanofiller concentrations, such as in Figure 4(c) and (d). The spherulite structures were transformed to imperfect fan-type structures with disordered regions. The increase in the disordered regions in both Figure 4(c) and (d) resulted in decreased mechanical properties, because mechanical properties depend on the amorphous phase in the spherulites.^{15,16} However, the planetary mill method generated mainly spherulitic supramolecular structures at all nanofiller concentrations, as shown in Figure 4(e)–(g). Furthermore, these images also show smooth supramolecular PNC structures and absence of NP agglomeration.

As shown in Figures 5 and 6, PNCs with 1.0 wt % SiO₂ were subjected to EDS. The spectra showed an irregular distribution of the NPs in the polymer matrix in the case of PNCs obtained with a paddle mixer. EDS analysis indicated that the NPs were localized in the boundaries (Figure 5, area 1) of the imperfect fan-type structure, in the disordered regions (Figure 5, area 3), and in the center of the spherulites (Figure 6, area 1). The highest concentration of NPs was observed in the disordered regions (Figure 5, area 3). Smaller

NPs exhibit a higher surface energy, and a high NP concentration results in ready aggregation and degrades the composite's mechanical properties. Compared with paddle mixing, joint mechanical activation promotes localization of the NPs only in the centers and boundaries of the spherulites, leading to a uniform distribution of NPs in the polymer matrix.

XRD was carried out to quantitatively characterize the crystalline structure of the PNCs. The XRD analysis indicated that UHMWPE crystallizes in the orthorhombic system. Unit cell parameters at equilibrium are $a = 0.74$ nm, $b = 0.493$ nm, and $c = 0.254$ nm. The planes for orthorhombic UHMWPE are (100) and (200).^{18,19} As shown in Figure 7, the XRD patterns of the composites are similar, with differences only in peak parameters such as broadening and intensity. The intensity of a peak corresponds to the phase content, and peak broadening is related to the crystallite size and microdistortions.²⁰ Thus, the NPs do not affect the unit cell parameters, but have an impact on the crystallinity of the composites, as well as the microdistortions and sizes of the crystallites. The presence of the NPs is significant in the crystallization process, as they affect the crystallization kinetics, and eventually change the crystallite dimensions.

The microstructural parameters, including the distortion level and sizes of coherent scattering regions (CSR), were evaluated from the XRD patterns by the Williamson–Hall (W–H) and Scherrer methods. The Scherrer method does not include contributions from the microdistortions to the peak broadening, in contrast to the W–H method, and hence, the difference between the CSR sizes calculated by the two methods was used to determine the contribution of microdistortions to the peak broadening.

Peak shapes were described by the Pearson VII function to determine the peak broadening. The XRD peaks were nearly Lorentzian, and consequently, the dependence between the

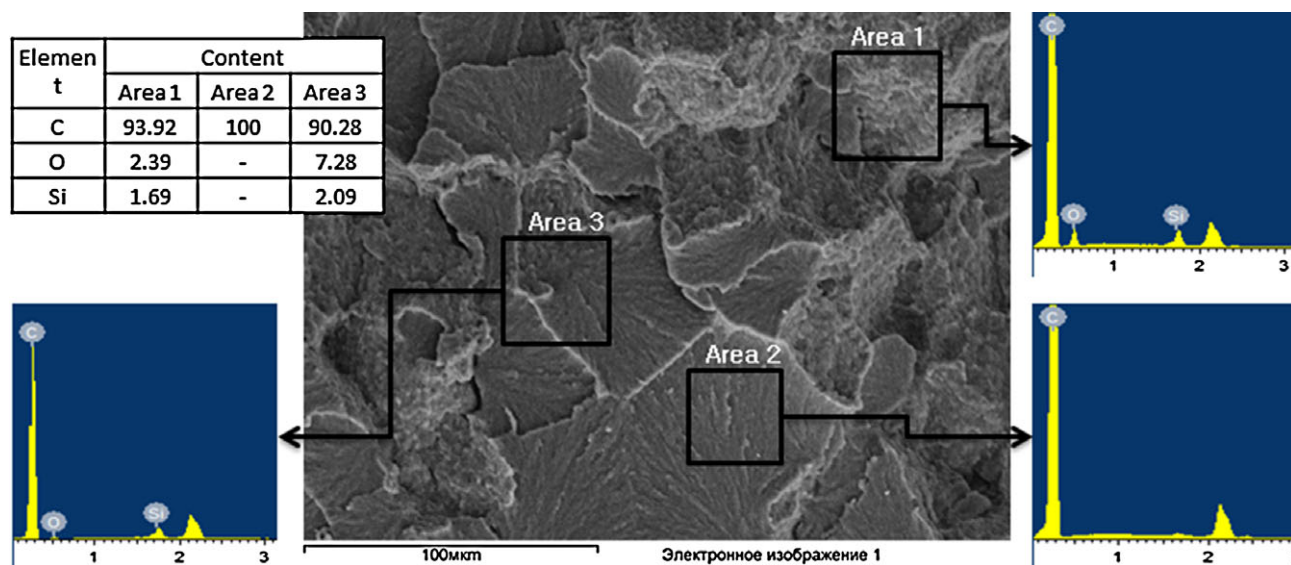


Figure 5. SEM image and EDS maps of UHMWPE + 1 wt % SiO₂ (paddle mixer).

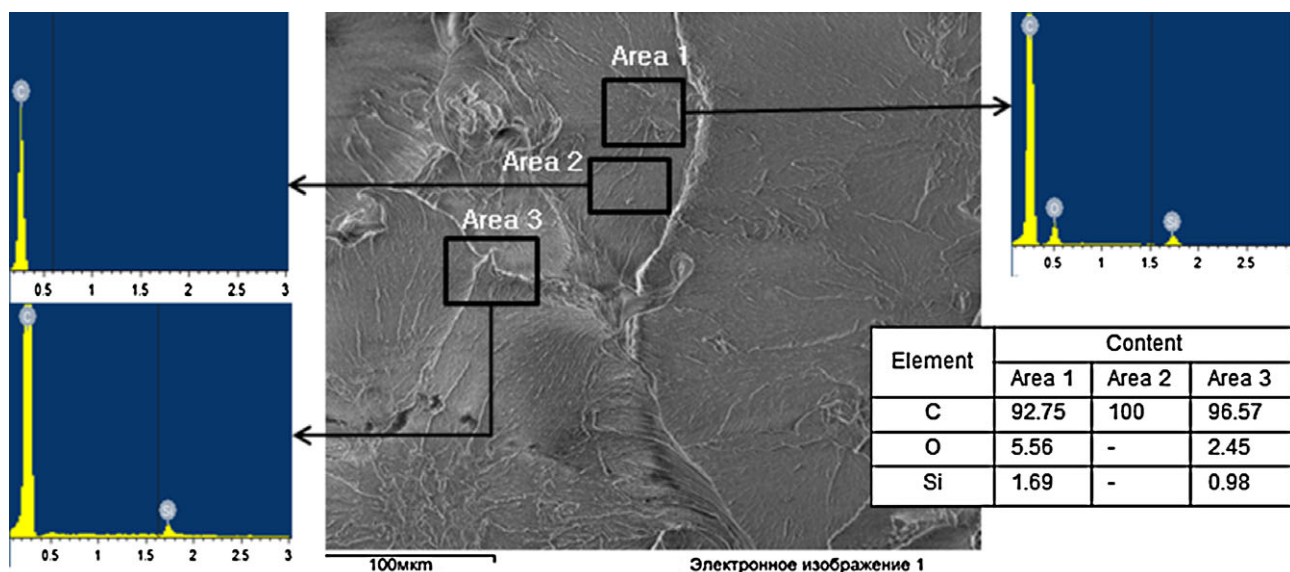


Figure 6. SEM image and EDS maps of UHMWPE + 1 wt % SiO₂ (planetary mill).

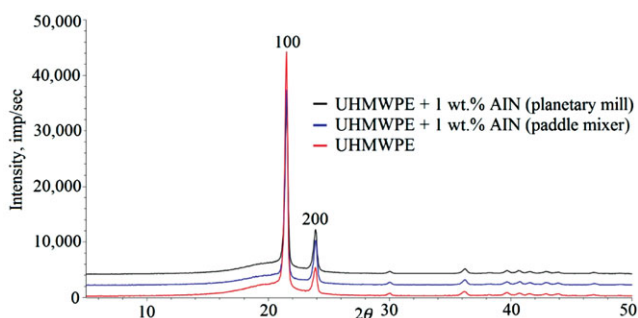


Figure 7. XRD patterns of UHMWPE and AlN composites.

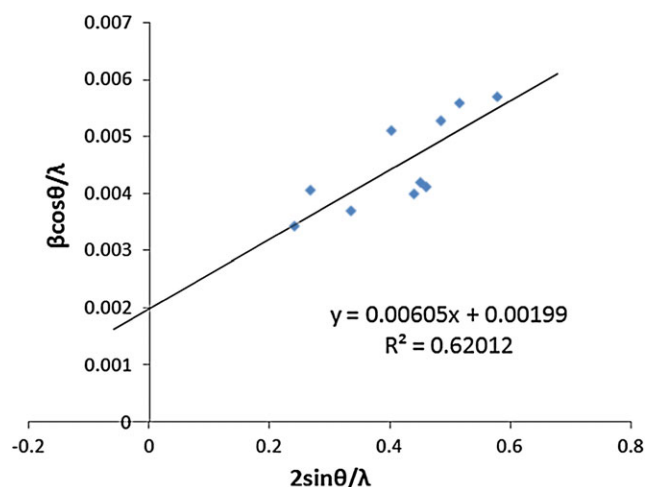


Figure 8. W–H graph of pristine UHMWPE, where $\epsilon = 6.05 \times 10^{-3}$, $D = 50$ nm.

integral half-width and the CSR size and distortion value was used in the W–H method, as shown below.²⁰

$$\beta = \frac{K\lambda}{D \cos \theta} + 2\epsilon \tan \theta$$

β is the physical broadening of the XRD peak, λ is the wavelength of the Cu K α radiation (1.54056 Å), K_S is the Scherrer constant (may be accepted as 1), D is the CSR size, θ is the Bragg angle, and ϵ is the microdistortion of the unit cells. The average D and ϵ (tangent of graph) were calculated from the linear function (Figure 8).

As shown in Table 2, the microdistortion decreased more with aluminum-based nanofillers than for silicon-based nanofillers. The average particle size of silicon oxide is about 20 nm, which promotes the transformation of the UHMWPE microstructure in the PNCs. The maximum mechanical properties were observed in PNCs with 0.1–0.5 wt % Si-based nanofillers and in samples with 1 wt % Al-based nanofillers. These observations can be attributed to the significant differences in specific area, bulk density, and crystallinity of the fillers.

The calculations of the crystallinity were carried out using the Crystallinity software package (Perkin Elmer, Seoul, Korea); the results are shown in Table 2. Changes in the crystallinity degree were observed when the polymer was filled by different NPs. The CSR size calculated by the W–H method decreased in samples obtained from the planetary mill for all types of fillers. The noticeable variation in the CSR sizes calculated by the two different methods indicates the presence of significant microdistortions in the microstructures of the PNCs. However, as shown in Table 2, the introduction of NPs into the polymer matrix decreased the microstrains in the crystalline structure in comparison with that in neat

Table 2. Structural parameters of UHMWPE and its PNCs by XRD.

Object	Mixing method	Crystallinity (%)	Size of CSR (W–H), nm	Size of CSR (Scherrer), nm	Microdistortion, $\times 10^{-3}$
UHMWPE	—	55	32	21	6.05
UHMWPE + 1 wt % Al_2O_3	Paddle mixer	51	49	23	4.86
	Planetary mill	48	32	28	1.08
UHMWPE + 1 wt % AlN	Paddle mixer	57	34	25	1.96
	Planetary mill	53	33	24	2.02
UHMWPE + 0.5 wt % Si_3N_4	Paddle mixer	57	40	24	3.38
	Planetary mill	59	37	25	2.56
UHMWPE + 0.5 wt % SiO_2	Paddle mixer	56	44	24	3.82
	Planetary mill	54	40	32	2.90

UHMWPE, which may provide an explanation for the improvement in the mechanical characteristics of the PNCs.

Conclusions

We fabricated PNCs with aluminum- and silicon-based nanofillers using a planetary mill and paddler mixer, and evaluated their mechanical characteristics such as tensile strength and elongation at break. The planetary mill was more effective for mixing than the paddle mixer, and prevented agglomeration of the NPs. Joint mechanical activation of the composite components with the planetary mill led to a more perfect supramolecular and crystalline structure in the PNCs. In addition, imperfect spherulites and disordered regions in the supramolecular structure of the PNCs decreased their mechanical properties.

Acknowledgments

This research was supported by the Internal Strategic Development Program of the North-Eastern Federal University, initiated by Rector Evgenia I. Mikhaylova; the Ministry of Education and Science of the Russian Federation for State Research Assignment (grants No. 11.512.2014/K and No. 1426); and the Head of the Republic of Sakha (Yakutia) (Grant No. 105-RG). The research in Korea was supported by the National Research Foundation of Korea (NRF2014K2A1A2048348).

References

- C. Sciancalepore, F. Bondioli, M. Messori, G. Barrera, P. Tiberto, P. Allia, *Polymer* **2015**, *59*, 278.
- A. A. Okhlopko, S. A. Sleptsova, *Bull. Korean Chem. Soc.* **2013**, *34*(5), 1345.
- I. V. Kirillina, L. A. Nikiforov, A. A. Okhlopko, S. A. Sleptsova, C. Yoon, J.-H. Cho, *Bull. Korean Chem. Soc.* **2014**, *35*(12), 3411.
- L. Hongtao, J. Hongmin, W. Xuemei, *Cryogenics* **2013**, *58*, 1.
- GUR Ultra-high molecular weight polyethylene (PE-UHMW), Ticona Catalog, USA. **2001**, p. 14.
- A. A. Aly, E. B. Zeidan, A. A. Alshennawy, A. A. El-Masry, W. A. Wasel, *World J. Nanosci. Eng.* **2012**, *2*, 32.
- B. J. Briscoe, A. K. Pogosian, D. Tabor, *Wear* **1974**, *25*, 19.
- S. M. Kurtz, *UHMWPE Biomaterials Handbook*, Elsevier, New York, **2009**, p. 63.
- D. Hannoche, M. Hamadouche, R. Nizard, P. Bizot, A. Meunier, L. Sedel, *Clin. Orthop. Relat. Res.* **2005**, *430*, 62.
- K. S. Morley, P. B. Webb, N. V. Tokareva, A. P. Krasnov, V. K. Popov, J. Zhang, C. J. Roberts, S. M. Howdle, *Eur. Polym. J.* **2007**, *43*(2), 307.
- O. V. Gogoleva, A. A. Okhlopko, P. N. Petrova, J. Frict, *Wear* **2014**, *35*(5), 383.
- S. Wannasri, S. V. Panin, L. R. Ivanova, L. A. Kornienko, S. Piriyaon, *Procedia Eng.* **2009**, *1*, 67.
- GOST 11262-80, *Plastics Tensile Strength Test Method*, USSR State Committee of Standards, Moscow, **1986**.
- L. Reimer, *Scanning Electron Microscopy: Physics of Image Formation and Microanalysis*, Vol. 17, Springer Science & Business Media, Berlin, Germany, **1998**.
- M. F. Butler, A. V. Donald, *J. Mater. Sci.* **1997**, *32*, 3675.
- P. B. Bowden, R. J. Young, *J. Mater. Sci.* **1974**, *9*, 2034.
- H. S. Khare, D. L. Burris, *Polymer* **2010**, *51*, 719.
- A. Peacock, *Handbook of Polyethylene: Structures: Properties, and Applications*, CRC Press, New York, USA, **2000**, p. 544.
- C. Vasile, M. Pascu, *Practical Guide to Polyethylene*, Smithers Rapra Press, Shawbury, **2008**, p. 188.
- D. Balzar, N. Audebrand, M. R. Daymond, A. Fitch, A. Hewat, J. I. Langford, A. Le Bail, D. Louër, O. Masson, C. N. McCowan, N. C. Popa, P. W. Stephens, B. H. Toby, *J. Appl. Crystallogr.* **2004**, *37*, 911.